

# Synthesis and characterization of Fe(III)-ion imprinted polymers (Fe-IIPs) as selective sorbents with Alizarin Red-S and 2-vinylpyridine

Neena Zakia<sup>1,1</sup>, M. Syaifudin Rizky Sumarsono<sup>1</sup>, Irma Kartika Kusumaningrum<sup>1</sup>, Nurlin Abu Samah<sup>2</sup>, and M. Bachri Amran<sup>3</sup>

<sup>1</sup>Chemistry Department, Universitas Negeri Malang, 65145 Malang East Java, Indonesia

<sup>2</sup>Faculty of Industrial Sciences and Technology, Universiti Malaysia Pahang Al Sultan Abdullah, 26300 Kuantan Pahang, Malaysia

<sup>3</sup>Chemistry Department, Institut Teknologi Bandung, 40132 West Java, Indonesia

**Abstract.** Iron (Fe) is an essential trace element that requires monitoring and removal when it acts as a pollutant. Previous studies have demonstrated limited selectivity in separating Fe(III) from complex sample matrices. To overcome these drawbacks, in this study Fe(III)-Ion Imprinted polymers (Fe-IIPs) were synthesized as selective sorbents with Alizarin Red-S as a ligand and 2-Vinylpyridine as a functional monomer. Bulk polymerization was carried out with Trimethylolpropane trimethacrylate (TMPTMA) as a crosslinker. Fe(III) ions were eluted with an HNO<sub>3</sub> solution to create the template. Non-Imprinted Polymers (NIPs) prepared without an imprinted ion, served as controls. The synthesized Fe-IIPs were characterized by FTIR (spectra), SEM (morphology), and EDX (elemental content). The effects of contact time, pH, and initial concentration were studied. Adsorption equilibrium was reached within 30 minutes. The maximum adsorption capacity of Fe-IIPs was 134.224 mg g<sup>-1</sup> at pH 5. The adsorption isotherm of Fe-IIPs conformed to the Langmuir model, while the kinetic adsorption data fitted the pseudo-second order model. The selectivity coefficient for Fe(III) ions relative to interfering ions exceeded unity, indicative of the imprinting effect.

## 1 Introduction

Iron (Fe) is an essential micronutrient that plays a crucial role in numerous biological and environmental systems. On the other hand, excessive or insufficient iron concentration can cause severe problems, both ecologically and physiologically. In environmental systems, monitoring and removal of Fe(III) ions from aquatic media is of increasing concern due to the discharge of various industrial wastes. Conventional methods for Fe(III) separation, such as precipitation, solvent extraction, and ion exchange, often suffer from poor selectivity, high operational cost, and the generation of secondary waste [1]. Therefore, the development of effective, selective, and environmentally friendly sorbent materials for Fe(III) recognition and removal has become a crucial area of research.

<sup>1</sup> Corresponding author: [neena.zakia.fmipa@um.ac.id](mailto:neena.zakia.fmipa@um.ac.id)

Several sorbents have been developed for Fe(III) separation, including activated carbon, zeolite, bentonite, chitosan, and cellulose [2]. However, these adsorbents have lack selectivity, resulting in poor adsorption of Fe(III) ions due to interference from other matrices in the solution. Sorbents with high selectivity properties, such as Ion Imprinted Polymers (IIPs), have been developed to overcome this limitation.

IIPs (Ion Imprinted Polymers) are a promising adsorbent material because it is designed to recognize specific ions. These polymers are synthesized via polymerization in the presence of a target ion (template), which produces specific binding cavities that are complementary to the target ion in terms of size, shape, and coordination environment to the target ion [3]. After template removal, these imprinted sites exhibit high selectivity toward the target ion, even in the presence of competing ions. IIPs provide better chemical stability, reusability, and adjustable selectivity than conventional ion-exchange resins or chelating compounds.

Selecting the right functional monomer and ligand is crucial for efficient IIP synthesis for Fe(III) ions. Ligands increase the adsorption capacity compared to their absence. For Fe(III), studied ligands include 8-Hydroquinoline, Gallic Acid, and Poly Eugenoxycetate [4-6]. Alizarin Red-S is an alternative ligand, able to form complexes with transition metals via hydroxyl and carbonyl groups [7]. 2-Vinylpyridine is chosen as the functional monomer due to its polymerizable vinyl group. This monomer also aids template formation between the ion-ligand complex and the crosslinker in Ion-Imprinted Polymers [3].

Combining Alizarin Red-S and 2-Vinylpyridine in the the synthesis of Fe(III)-Ion Imprinted Polymers (Fe-IIPs) is desired to produce a selective sorbent with high binding affinity and selectivity toward Fe(III) ions. Therefore, this study aims to synthesis and characterize Fe-IIPs using Alizarin Red-S and 2-Vinylpyridine as ligand and functional monomer, respectively, to develop a novel and selective sorbent for Fe(III) ions. In this study, it is anticipated that the IIPs material can be effectively utilized for the preconcentration, separation, or removal of Fe(III) from complex matrices, thereby contributing to advancements in analytical and environmental applications.

## 2 Experimental

### 2.1 Chemical reagents

The chemicals used in this study were pro analysis reagent grade, Iron(III) chloride hexahydrate (Merck), 2-Vinylpyridine (Sigma Aldrich), Alizarin Red-S (Merck), Trimethylolpropane trimethacrylate (Shandong Fan Tai Fine Chemical Biotechnology), Benzoyl Peroxide (Merck), Acetonitrile (Merck), Nitric acid (Smartlab), Nickel(II) nitrate hexahydrate (Merck), Copper(II) sulphate pentahydrate (Merck), silicone oil, and aquadest.

### 2.2 Instrumentation

An analytical balance (Shimadzu ATX224) with an accuracy of 0.0001 grams, water bath shaker (Eyela Uni Thermo Shaker NTS-1300), oven (Mettler), and a Mettler-Toledo pH meter. An atomic Absorption Spectrophotometer (Thermo Fischer Scientific iCE 3000) was used for measuring Fe(III) ion concentration. Fourier transform infrared (FT-IR) spectra were recorded using Shimadzu IR Prestige 21 over the wave number range 4000-400  $\text{cm}^{-1}$ . The surface morphology, size, shape, and atomic composition were examined by Scanning Electron Microscope (SEM)-Energy Dispersive X-Ray (EDX) FEI Inspect-S50.

### 2.3 Synthesis of Fe(III)-Ion Imprinted Polymers (Fe-IIPs)

The synthesis of Fe(III)-Ion Imprinted Polymers (Fe-IIPs) was prepared by the bulk polymerization technique. Synthesis of Fe-IIPs using Alizarin Red-S, 2-Vinylpyridine, Trimethylolpropane trimethacrylate (TMPTMA), Benzoyl Peroxide (BPO), and acetonitrile, respectively, as ligand, functional monomer, crosslinker, initiator, and porogen. Synthesis is carried out through several stages, namely complex formation, prepolymerization, polymerization, and template removal or leaching to form a mold. The mole ratio between template, ligand, monomer, and crosslinker is 1:1:4:20 mmol. The initial stage is the formation of a complex between Fe(III) and Alizarin Red-S. Based on initial studies, the mole ratio of Fe(III) to Alizarin Red-S was 1:1. Fe(III) ions, used as a template (0.1 mmol), and Alizarin Red-S (0.1 mmol) were mixed in 5 mL of Acetonitrile solvent and stirred for 15 minutes. Prepolymerization step accomplished with mixing the Fe(III)-Alizarin Red-S complex and 2-Vinylpyridine (0.4 mmol), then stirring for 2 hours to maximize template formation. The polymerization step was achieved by adding TMPTMA (2 mmol) and BPO (250 mg), then stirred until homogeneous. After that, the polymerization process is carried out by heating the mixture in a silicone oil bath for 6 hours and stirring constantly at a temperature of 60°C. Then, the IIPs that have been formed are dried in an oven for 2 hours at a temperature of 60°C. The next stage is leaching using 2 M HNO<sub>3</sub> solvent. The synthesized Fe-IIPs are dried in an oven at 60°C. The synthesized Fe-IIPs material was ground and sieved with a 60 mesh sieve for further physical characterization and performance evaluation.

### 2.4 Physical characterization

FT-IR Spectrometry was utilised to characterize the functional groups of Fe-IIPs and non-imprinted polymers (NIPs) in the wavenumber range of 4000-400 cm<sup>-1</sup>. The surface morphology of IIPs before and after leaching was observed using SEM-EDX instrumentation, which was then compared with control NIPs. The presence of Fe(III) ion templates in IIPs after leaching was confirmed using the EDX instrument.

### 2.5 Batch sorption experiment

The adsorption effectiveness of Fe-IIPs was evaluated through batch binding analysis. The influences of pH, interaction time, and optimum adsorption capacity were investigated using binding analysis.

The batch experimental procedure was examined for the adsorption of Fe(III) from an aqueous solution. 10 mg of Fe-IIPs was placed in a vial and add 25 mL of Fe(III) solution 10 mg L<sup>-1</sup>. The mixture was shaken at 150 rpm for 24 hours of interaction. The filtrate was separated from the sorbent, and measured by AAS. The same procedure was also carried out with NIPs. The adsorption capacity was calculated as follows:

$$Q_e = \frac{v(C_o - C_e)}{w} \quad (1)$$

where  $Q_e$  is the adsorption capacity (mg g<sup>-1</sup>),  $v$  is the volume of solution (L),  $C_o$  and  $C_e$  are the initial and equilibrium concentration of Fe(III) solution, respectively, and  $w$  is the sorbent mass (g).

#### 2.5.1 Effect of interaction time on sorption

10 mg of Fe-IIPs was placed into a vial and incubated with 25 mL of Fe(III) solution (10 mg L<sup>-1</sup>). The adsorption process was evaluated with a time variation of 15, 30, 60, 90, and 120

min, respectively, and shaken in a 150 rpm shaker at room temperature. Subsequently, the mixture was decanted and measured for Fe(III) ion concentration by AAS. NIPs were also examined by the same procedure.

### 2.5.2 pH optimization

The effect of pH on sorption was evaluated by contacting 10 mg of Fe-IIPs and 25 mL Fe(III) solution ( $10 \text{ mg L}^{-1}$ ) at varying pH value 3, 4, 5, and 6, respectively, which was placed into a vial. The adsorption process was carried out using a shaker at 150 rpm for optimum time. The filtrate was separated from the sorbent, and measured by AAS. NIPs were also examined by the same procedure.

### 2.5.3 Determination of maximum adsorption capacity

To determine the maximum adsorption capacity of the sorbent, 10 mg of Fe-IIPs was placed in a vial and then interact with 25 mL Fe(III) solution at optimum interaction time and pH. The mixture was shaken in a 150 rpm shaker with various concentrations of Fe(III) for 25, 50, 100, 125, and  $150 \text{ mg L}^{-1}$ . The filtrate was separated from the sorbent, and measured by AAS. NIPs were also examined by the same procedure.

### 2.5.4 Kinetic Study

The study of adsorption kinetic was examined by testing the data using pseudo-first order model and pseudo-second order model, which follow the equation:

$$\log \log (Q_e - Q_t) = \log Q_e - \frac{k_1}{2,303} t \quad (2)$$

$$\frac{t}{Q_t} = \frac{1}{k_2 Q_e^2} + \frac{1}{Q_e} t \quad (3)$$

where  $Q_e$  is the adsorption capacity at the equilibrium condition ( $\text{mg g}^{-1}$ ),  $Q_t$  is the adsorption capacity of  $t$  time ( $\text{mg g}^{-1}$ ),  $k_1$  and  $k_2$  are the adsorption rate constant for pseudo-first order ( $\text{min}^{-1}$ ) and pseudo-second order ( $\text{g mg}^{-1} \text{min}^{-1}$ ) kinetics model, respectively.

### 2.5.5 Adsorption Isotherm

Adsorption isotherms were evaluated using Langmuir and Freundlich model isotherm. The Langmuir isotherm are expressed as the Eq. 7, and Freundlich adsorption isotherm models are expressed in the Eq. 5.

$$\frac{C_e}{Q_e} = \frac{1}{Q_m \cdot K_L} + \frac{C_e}{Q_m} \quad (4)$$

$$\log Q_e = \log K_f + \frac{1}{n} \log \log C_e \quad (5)$$

where  $C_e$  is the equilibrium concentration of a metal ion,  $Q_e$  is the adsorption capacity of the sorbent,  $Q_m$  is the maximum adsorption capacity of the sorbent, and  $b$  is Langmuir constant. While in the Freundlich isotherm,  $n$  and  $K_f$  are the Freundlich constants.

### 2.5.6 Selectivity

The selectivity of Fe-IIPs sorbent to Fe(III) ion was evaluated by interacting 10 mg of the sorbent in 25 mL of single and binary mixtures of Fe(III), Cu(II), and Ni(II) metal ions at the optimum concentration and conditions that had been carried out. Fe(III) selectivity in the presence of other competing ions reveals the Fe-IIPs sorbent's ability to recognise ions. The selectivity of the Fe-IIPs and NIPs was analyzed using the equation:

$$K_d = \frac{v(C_o - C_e)}{C_o w} \quad (6)$$

$$k = \frac{K_d Fe}{K_d Me} \quad (7)$$

$$k' = \frac{k [IIPs]}{k [NIPs]} \quad (8)$$

where  $K_d$ ,  $k$ , and  $k'$  represent the distribution ratio, selectivity coefficient, and relative selectivity coefficient, respectively.  $K_d Fe$  and  $K_d Me$  show the distribution ratio for the Fe(III) ion and the other selected competitive metal ion respectively.

## 3 Results and discussion

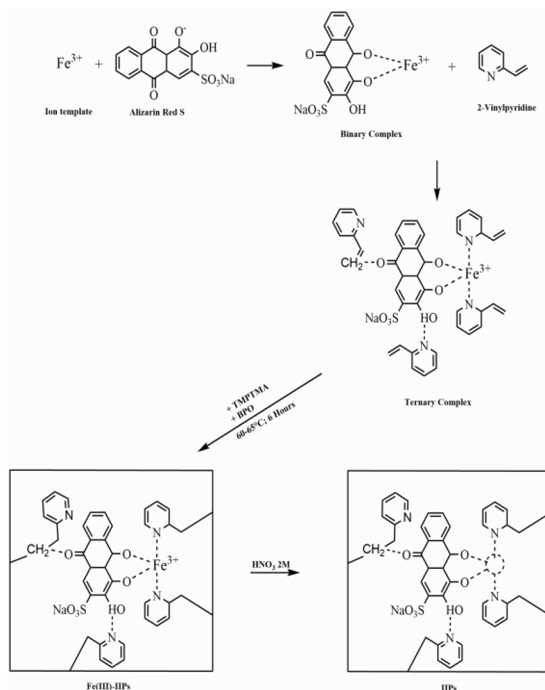


**Fig. 1.** Schematic procedures of complex-based Fe-IIPs synthesis (modified from research by Behbahani et al. [8])

The synthesis of Fe-IIPs encompasses multiple stages, including the establishment of a complex between ions and ligands, followed by prepolymerization, polymerization, and ultimately the generation of a template through the leaching of the complex molecules. Fe-

IIPs synthesis proceeds through the complex formation stage between Fe(III) ion and Alizarin Red-S as ligand, to create the structure of the template.

Complexation was accomplished for 2 hours to maximize the coordinate covalent bonds formed between Fe(III) ions with pyridine groups in 2-Vinylpyridine (2-VP) and Fe(III) ions with hydroxyl and carbonyl groups in Alizarin Red S to form a ternary complex [3]. The 2-Vinylpyridine was chosen as a functional monomer because it has good thermal stability properties [3]. In addition, the presence of nitrogen atoms in 2-VP makes it weakly basic, and its lone electron pairs can interact with metals. Meanwhile, Alizarin Red-S was chosen as a complexing ligand because Alizarin Red S has a hydroxyl group that has a lone electron pair that can bond with Fe(III) ions [7].

The prepolymerization stage, which involves the interaction of Fe(III)-Alizarin complexes with functional monomers via a self-assembly mechanism, is then completed. The Fe(III)-alizarin complex and functional monomers are stabilised in the polymer during polymerization, and this complex is enclosed by numerous crosslinkers (TMPTMA) to create a stiff three-dimensional network. Leaching the complex to create a template is the next step in the synthesis process. Following leaching, the polymer will create an empty cavity with particular recognition sites based on the abandoned complex's structural form. The synthesis procedure is illustrated in Fig. 1.

### 3.1 Physical characterization of sorbents

#### 3.1.1 FTIR analysis

The Fourier Transform Infrared (FTIR) analysis was used to evaluate the functional groups in Fe-IIPs and NIPs. The FTIR spectra for Fe-IIPs before and after the leaching process, and NIPs are shown in Fig. 2.

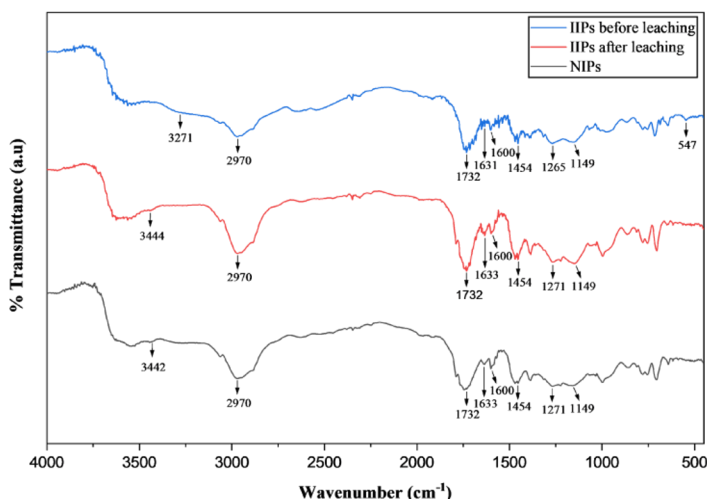


**Fig. 2.** FTIR spectra of IIPs before leaching (blue curve), after leaching (red curve), and NIPs (black curve)

The successful formation of IIPs and NIPs can be characterized by the absence of C=C bond stretching vibrations in the vinyl group, which is a typical peak in 2-Vinylpyridine at a wave number of around 1640 cm<sup>-1</sup>. The disappearance of C=C bond stretching vibrations in the vinyl group confirms the perfection of the polymerization results, where the vinyl group of 2-Vinylpyridine has formed a polymer chain. In IIPs before and after leaching, there is a

significant difference in C-N bond stretching vibrations. In IIPs before leaching, a band of C-N bond stretching vibrations was observed at  $1265\text{ cm}^{-1}$ , which shifted to  $1271\text{ cm}^{-1}$  in IIPs after leaching.

This shift indicates an interaction between nitrogen from the C-N group in pyridine and Fe(III) ion in IIPs before leaching. When the IIPs are successfully leached, the stretching vibration of the C-N bond of pyridine experiences a shift in the same wave number as NIPs [9].

In IIPs before leaching and after leaching, differences were observed in the typical peaks of the O-H bond stretching vibration and the C=O stretching vibration of Alizarin Red S. In IIPs before leaching, there was a broad band of the O-H bond stretching vibration at a wave number of  $3271\text{ cm}^{-1}$ , which shifted to  $3444\text{ cm}^{-1}$  in IIPs after leaching. While the C=O bond stretching vibration was observed with a band produced by IIPs before leaching at a wavenumber of  $1631\text{ cm}^{-1}$  shifted to  $1633\text{ cm}^{-1}$  in IIPs after leaching. This shift indicates an interaction between oxygen from the O-H and C=O groups in Alizarin Red S, which interacts with Fe(III) ion in IIPs before leaching. According to research conducted by Behbahani et al. [8], the shift in wave numbers in the O-H and C=O groups indicates the presence of new bonds in IIPs before leaching, which are formed between oxygen atoms and metal ions that have higher energy compared to the bonds that have been broken in IIPs after leaching. The interaction between the O atoms in the hydroxyl and carbonyl groups of Alizarin Red S with Fe(III) ions is supported by the appearance of a weak, sharp band at  $547\text{ cm}^{-1}$ , which is a typical peak of the stretching vibration of the Fe-O bond in IIPs before leaching. Based on research conducted by Ara et al. [4] stated that the typical peak of the Fe-O bond appears at  $580\text{ cm}^{-1}$ . Meanwhile, in IIPs after leaching, no typical Fe-O peak was observed at a wavenumber around  $500\text{-}600\text{ cm}^{-1}$ , which indicates that the Fe(III) ion in IIP after leaching were successfully completely removed.

### 3.1.2 SEM-EDX Analysis

The measurement results from SEM for Fe-IIPs before leaching, Fe-IIPs after leaching, and NIPs are shown in Fig. 3. The results of elemental analysis from Energy Dispersive X-ray (EDX) measurement for Fe-IIPs before and after leaching, and NIPs are shown in Table 1.

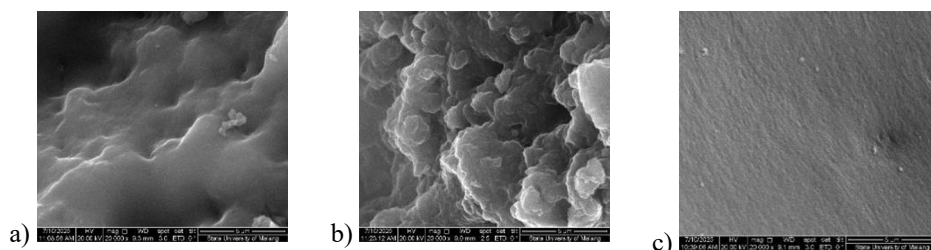


**Fig. 3.** The SEM images (20,000x magnification) of (a) Fe-IIPs before, (b) Fe-IIPs after, (c) NIPs

**Table 1.** Elemental analysis from SEM-EDX for all the sorbents

Sorbent	%Mass				%Atom			
	C	O	Cl	Fe	C	O	Cl	Fe
Fe-IIPs before	77.97	21.28	0.49	0.25	82.80	16.97	0.18	0.06
Fe-IIPs after	80.68	18.44	0.88	-	85.09	14.60	0.31	-
NIPs	80.29	19.71	-	-	84.44	15.56	-	-

The morphology of the three sorbents showed differences in surface structure. In NIPs, the surface morphology was smoother and more compact compared to IIPs before and after leaching. IIPs after leaching exhibited a surface morphology structure that tended to be more open and produced cavities compared to IIPs before leaching. This open morphology and the presence of cavities indicate a wider adsorbent surface and the potential to provide active sites that can be used to bind with Fe(III) ions [10]. However, the surface texture of IIPs after leaching tends to be rough, which is possibly due to the grinding process after the leaching process. The synthesis of IIPs and NIPs using the functional monomer 2-Vinylpyridine produces hard materials, thus requiring grinding. This grinding process can cause the specific cavities formed to be damaged by physical treatment, thus becoming non-selective sites, and can reduce the performance of IIPs [3]. Meanwhile, the surface of IIPs before leaching tends to be closed, which indicates that the cavities are still closed, because there has not been a template removal process.

The presence of Cl elements detected in SEM–EDX analysis most likely originates from the use of FeCl<sub>3</sub> as a template ion source during the IIPs synthesis stage. In IIPs synthesis, Fe(III) coordinates with alizarin through phenolic and carbonyl groups, forming a relatively strong Fe-alizarin complex during the template stage. When FeCl<sub>3</sub> is used as a Fe(III) source, Cl<sup>-</sup> ions act as counterions to balance the complex charge. This condition is also influenced by the use of Fe-IIPs components, namely ligands (Alizarin) and functional monomers (2-Vinylpyridine).

Some of these Cl<sup>-</sup> ions can be physically trapped or weakly bound within the polymer network or around the imprint sites with the Fe-alizarin complex during the polymerization process, so they are not completely released during the leaching stage. In addition, the 2-vinylpyridine monomer has a nitrogen atom on the pyridine ring that is easily protonated under acidic conditions, both during the synthesis stage and leaching with HNO<sub>3</sub>. In the protonated state, the pyridine group can attract and stabilize Cl<sup>-</sup> ions through electrostatic interactions [11]. These interactions are not covalent, but are strong enough to retain some Cl<sup>-</sup> within the polymer matrix, especially at low pH.

Although HNO<sub>3</sub> is effective in removing Fe(III) ions, Cl<sup>-</sup> ions can remain on the surface or be trapped in the mold cavities, especially if they are weakly associated with protonated functional groups, so that Cl<sup>-</sup> is not always completely eluted. This phenomenon explains that the Cl<sup>-</sup> signal is still detected even though the leaching process does not involve hydrochloric acid.

From a sorbent performance perspective, the presence of Cl is closely related to the pH effect. At low pH, functional groups such as -OH or -NH in IIPs are protonated, thus attracting Cl<sup>-</sup> ions through electrostatic interactions [11]. This condition can potentially cause a charge screening effect or competition with target ions, which can temporarily reduce the availability of active sites. However, when the pH is increased, deprotonation of the functional groups occurs, allowing Cl<sup>-</sup> ions to be easily released and no longer affecting the accessibility of the imprint site. Therefore, the presence of Cl detected does not indicate contamination or failure of the leaching process, but rather is a logical consequence of using FeCl<sub>3</sub> as a template precursor and the acid-base behavior of the polymer matrix.

The existence of Fe(III) in the sorbent after leaching is compared to the sorbents prior to leaching, and NIPs, the polymer control, are analyzed using EDX to assess the effectiveness of leaching to create a mold. According to the EDX data, the Fe element was not found in NIPs. This indicates that NIPs, as a control, do not contain the target ion. In Fe-IIPs before leaching, the presence of Fe was observed, while in IIPs after leaching, the presence of Fe was no longer found. In IIPs before leaching, it indicates that Fe as a template-forming ion is already present in IIP, while after leaching indicates the success of the leaching process to generate a mold [5].

## 3.2 Rebinding study

### 3.2.1 Effect of interaction time

Determination of the optimum interaction time for Fe(III) adsorption in 10 mg Fe-IIPs at a concentration of  $10 \text{ mg L}^{-1}$  Fe(III) solution is shown in Fig. 4. The initial stage of the binding process was rapid; as interaction time increased, the adsorption rate steadily decreased. Initially, specific cavities were empty, but over time, these filled with Fe(III) ions, leading to increased adsorption capacity. As more cavities were occupied, however, the amount adsorbed increased less significantly, making longer interaction times less efficient [10]. While the time of 15 minutes and 30 minutes the difference in adsorption capacity is quite large at around  $1.30 \text{ mg g}^{-1}$ . Therefore, the interaction time of 30 minutes was chosen as the optimum time for interaction between the adsorbent and the adsorption interaction time. The specific, high-affinity cavities in IIPs shorten the required interaction time with Fe(III) ions, while NIPs, lacking such cavities, exhibit lower capacity and need longer optimum interaction times.

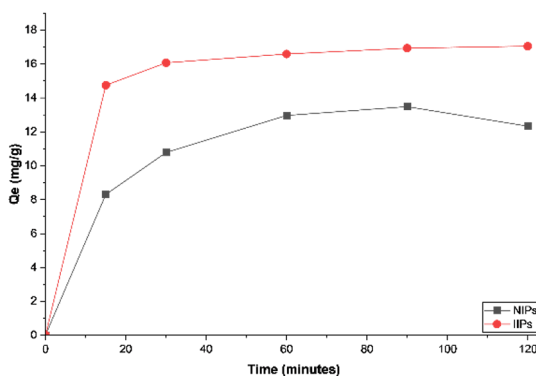


**Fig. 4.** The effect of interaction time on adsorption capacity ( $Q_e$ ) for Fe-IIPs and NIPs

### 3.2.2 Effect of pH

The pH influence on adsorption of Fe(III) ions on Fe-IIPs and NIP is shown in Fig. 5. The highest binding capacity of Fe(III) on Fe-IIPs was reached at pH 5. The pH condition will affect the ability of the adsorbent functional groups that play a role in the active site of Fe(III) ion binding.

The adsorption capability tends to increase at pH 3-5 and decrease at pH 6. Neutral solution conditions cause a tendency for the adsorption capacity to decrease because Fe(III) is easily hydrolyzed to  $\text{Fe}(\text{OH})_3$ , compared to its ionic form [5]. At pH below 3, changes in the chemical structure of the Alizarin ligand are possible, causing the Fe(III)-Alizarin complex to be unstable and not compatible with the Fe-IIPs template, resulting in a decrease in its adsorption capacity [12].

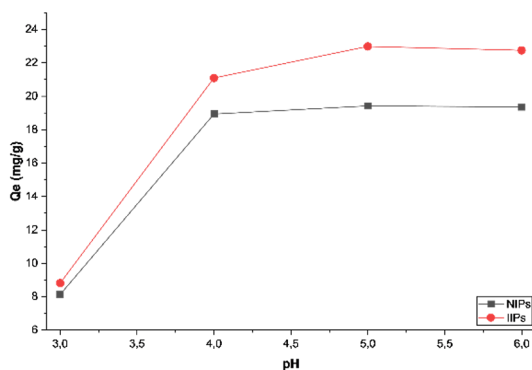


**Fig. 5.** The effect of pH on adsorption capacity ( $Q_e$ ) for Fe-IIPs and NIPs

### 3.2.3 Determination of maximum adsorption capacity

The binding capacity of the Fe-IIPs have been evaluated in equilibrium rebinding batch experiment. The experiment was performed by varying the initial concentration of Fe(III) solution. The curve of the effect of the concentration of Fe(III) solution on the maximum adsorption capacity of sorbents is shown in Fig. 6. The adsorption capacity of Fe-IIPs was  $134.224 \text{ mg g}^{-1}$ , while NIPs have adsorption capacities of  $127.863 \text{ mg g}^{-1}$ .

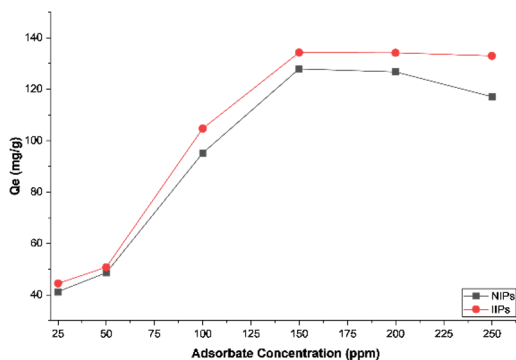


**Fig. 6.** Effect of initial concentration on adsorption capacity of Fe-IIPs and NIPs

The binding capacity of Fe(III) was shown to increase as the initial concentration of Fe(III) increased and achieved adsorption equilibrium. The mass transfer driving force increases with the rise of Fe(III) concentration and improves the adsorption capacity. The findings show that at greater concentration, the Fe-IIPs were approaching saturation. Fe(III) ions are more readily adsorbed in imprinted polymers (Fe-IIPs) than in NIPs, that not have the template. Furthermore, reusability testing over multiple adsorption-desorption cycles is highly recommended to assess the durability and potential practical applications of the adsorbent.

The use of Alizarin Red-S as a ligand provides advantageous to the adsorption of Fe(III) at optimum of interaction time and pH. Alizarin Red-S undergoes deprotonation, allowing for stronger and more stable interactions with Fe(III) ions, resulting in a dense and perfect polymer, thus enabling the formation of the desired template. The shape, size, degree of coordination, and charge of metal ions are the mechanisms underlying the memory effects,

which result in strong interactions with metal ions that have ligands and a higher adsorption capacity [3].

Compared to other sorbents, IIPs have a high capacity due to their suitable shape and size. Research conducted by Bakalár et al. [13] reported that zeolite-micro 20 was only capable of adsorbing Fe(III) with an adsorption capacity of 10.19 mg/g. This is due to the non-specific and non-selective pore shape and size of the zeolite, resulting in less than optimal Fe(III) ion adsorption.

### 3.3 Kinetic study

The kinetics adsorption curves are shown in Fig. 7 and the kinetic parameters are presented in Table 2.

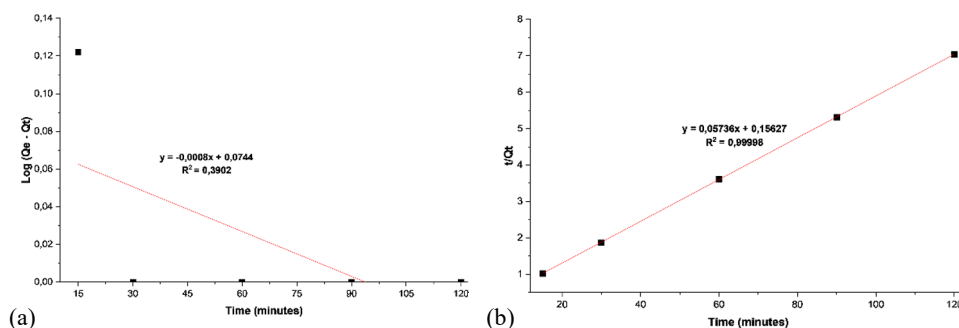


**Fig. 7.** (a) Pseudo first order and (b) pseudo-second order kinetic models of Fe-IIPs

**Table 2.** Pseudo order kinetic parameters of 1<sup>st</sup>-order and 2<sup>nd</sup>-order on Fe-IIPs sorbent

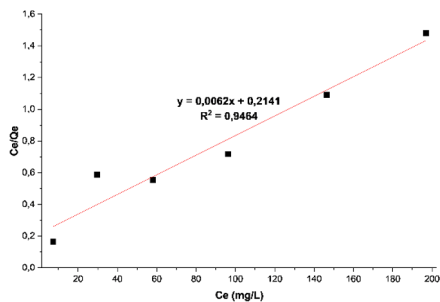
Sorbent	Pseudo-first order			Pseudo-second order			$Q_e \text{ exp}$
	$K_1$	$R^2$	$Q_e \text{ cal}$	$K_2$	$R^2$	$Q_e \text{ cal}$	
Fe-IIPs	0.003	0.3902	1.187	0.021	0.9999	17.435	16.076

According to the determined results, the correlation coefficient ( $R^2$ ) values of pseudo-second order model for Fe-IIPs are greater than those of the pseudo-first model. In the pseudo-second order model, the obtained equilibrium adsorption capacity ( $Q_e \text{ cal}$ ) values are near to the experimental data ( $Q_e \text{ exp}$ ). This result indicate that the adsorption kinetics of Fe(III) on Fe-IIPs follow the pseudo-second order kinetic models.

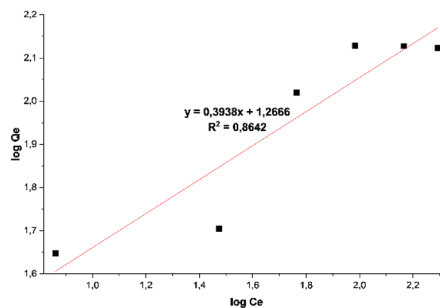
Pseudo-second order adsorption kinetics assumes that the adsorption that occurs in Fe-IIPs towards Fe(III) ions is controlled by chemisorption. The nature of Fe-IIPs that create imprinted binding sites during polymer synthesis. The polymers form specific and tailored binding cavities originating from the compound of Fe-IIPs, namely functional monomers (2-VP), complexing ligand (Alizarin Red-S), and spatially organized donor groups (hydroxyl, carbonyl, and pyridine groups), that create strong coordination bonds with Fe(III) [3]. Furthermore, the adsorption process is governed by Fe(III) ions and the chemically functionalized binding site. The adsorption process is controlled by the ion properly orienting itself and interacting with specific functional groups within the cavity to form a strong chemical bond [6]. As a result, the system approaches equilibrium gradually, which indicates slower chemisorption, rather than physical diffusion. This mechanistic behavior is consistent with pseudo-second-order kinetics, which describes processes dominated by chemical interactions.

### 3.4 Adsorption isotherm

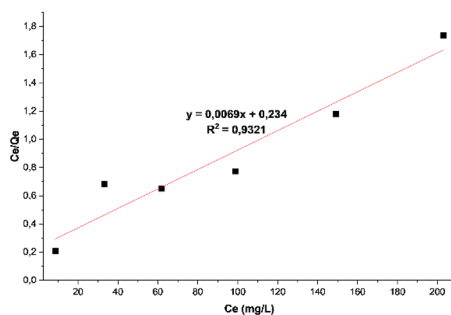
Adsorption isotherms were analyzed using Langmuir and Freundlich model isotherm. The Langmuir isotherm are expressed as the Eq. 4, and Freundlich adsorption isotherm models are expressed in the Eq. 5. The fitting results are given in Fig. 8 and Table 3.



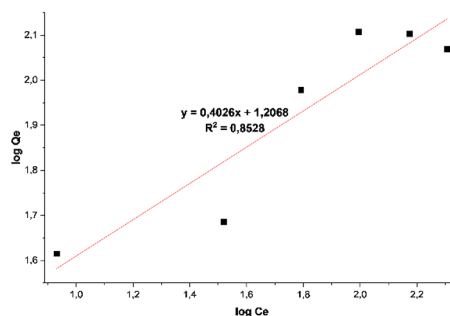
(a) Langmuir isotherm of Fe-IIPs



(b) Freundlich isotherm of Fe-IIPs



(c) Langmuir isotherm of NIPs



(d) Freundlich isotherm of Fe-IIPs

**Fig. 8.** Langmuir and Freundlich isotherm models of Fe-IIPs and NIPs

The curve shows the  $R^2$  value is 0.946 and follows the Langmuir isotherm model. Meanwhile, from the Table, it can be seen that the value of each parameter in the Fe-IIPs sorbent exhibits that the calculated  $Q_m$  value in the Langmuir isotherm adsorption model is close to the  $Q_m$  value obtained, namely  $134.224 \text{ mg g}^{-1}$  for Fe-IIPs. Thus, the Fe-IIPs sorbent follows the Langmuir isotherm model, which describes monolayer adsorption on the sorbent surface. This indicates that adsorption occurs on a homogeneous surface, while the Freundlich model assumes adsorption occurs on a heterogeneous or multilayer surface [10]. BET analysis is required to determine the porosity and surface area of the adsorbent for future experiments.

**Table 3.** Langmuir and Freundlich isotherm model parameters on Fe-IIPs and NIPs

Sorbent	Adsorption Model					
	Langmuir			Freundlich		
	$Q_m$ ( $\text{mg g}^{-1}$ )	$K_L$	$R^2$	$n$	$K_F$	$R^2$
Fe-IIPs	161.290	0.029	0.946	2.539	18.476	0.864
NIPs	144.927	0.029	0.932	2.484	16.099	0.853

### 3.5 Selectivity

The selectivity of Fe-IIPs towards Fe(III) in the presence of Cu(II) and Ni(II). Although both ions have different ionic radii and charges, these two ions are used due to the HSAB theory; they are classified as borderline hard and soft acids that are able to interact strongly with pyridine, which is a borderline base and can interfere with the adsorption process of Fe(III) ions. The influence of selectivity was carried out on other ions (Cu(II) and Ni(II)), with single and binary solution models, were shown in Fig. 9 (single solution) and Fig. 10 (binary solution). Table 4 shows the distribution coefficient ( $K_d$ ), relative selectivity coefficient ( $k'$ ), and the selectivity coefficient ( $k$ ) for the Fe-IIPs and NIPs.

**Table 4.** Selectivity on Fe-IIPs in single and binary solution

Cation	Single Solution			Binary Solution			
	Fe <sup>3+</sup>	Cu <sup>2+</sup>	Ni <sup>2+</sup>	Fe(III)/Cu(II)		Fe(III)/Ni(II)	
				Fe <sup>3+</sup>	Cu <sup>2+</sup>	Fe <sup>3+</sup>	Ni <sup>2+</sup>
$K_d$ Fe-IIPs (L g <sup>-1</sup> )	0.918	0.585	0.387	1.947	1.689	2.089	1.561
$K_d$ NIPs (L g <sup>-1</sup> )	0.809	0.597	0.485	1.832	1.681	1.650	1.339
$k$ Fe-IIPs		1.569	2.372		1.153		1.338
$k$ NIPs		1.355	1.668		1.089		1.232
$k'$ Fe-IIPs/NIPs		1.157	1.422		1.059		1.086

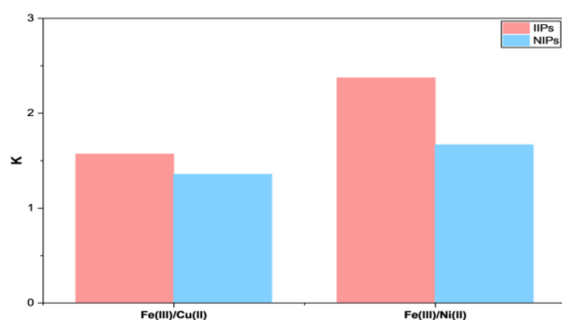


**Fig. 9.** Selectivity coefficient of Fe-IIPs in single solution

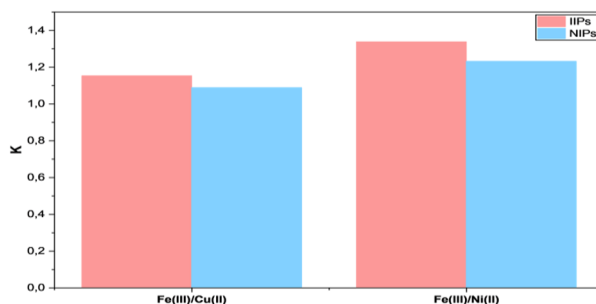


**Fig. 10.** Selectivity coefficient of Fe-IIPs in binary solution of Fe(III)/Cu(II) and Fe(III)/Ni(II)

The distribution coefficient of Fe(III) ions in Fe-IIPs is greater than that of Cu(II) and Ni(II) ions. In single solutions, Cu(II) and Ni(II) ions are not well adsorbed into the Fe-IIPs template. Cu(II) and Ni(II) ions can each be adsorbed, but are actually distributed within the polymer through non-specific sites. This is demonstrated by the  $K_d$  value of NIPs, which indicates that Cu(II) and Ni(II) ions do not actually enter the specific cavity (template) but

are adsorbed through non-specific sites, that functional groups other than those present in the template.

In binary solutions, Fe remains superior, being well distributed into the template, while both Cu(II) and Ni(II) are almost not distributed within the template in Fe-IIPs. The distribution coefficient in binary solutions increases compared to single solutions for each species. This is possible due to the interaction of metal ions with non-specific sites present in the grinding. Grinding in the post-leaching process can affect the surface morphology, resulting in the destruction of specific sites into non-specific sites [3]. The increased distribution coefficient in this binary solution can be made possible by the synergy effect. The synergy effect in the adsorption process describes an increase in the adsorption capacity for a mixture of ions compared to a single ion in solution. The synergy effect occurs when the presence of two types of metal ions does not interfere with each other, but instead triggers an increase in adsorption capacity [14]. The interaction between these ions allows for an increase in the driving force for entering specific cavities, resulting in the opening of other active sites that were initially difficult to enter, becoming more open to be bound by metal ions [15]. These findings suggest that because of the imprinted ion template in the polymer sorbent, Fe-IIPs has a greater capacity to recognise Fe(III).

## 4 Conclusion

Fe(III)-Ion Imprinted Polymers (Fe-IIPs) have been successfully synthesized for use as sorbents to remove Fe(III) ions, by bulk polymerization, that using Fe(III) ions with Alizarin Red-S ligands as a template, and 2-Vinylpyridine as a functional monomer, with Trimethylolpropane trimethacrylate as a crosslinker. Adsorption of Fe(III) on Fe-IIPs was obtained at pH 5 and at 30 min of interaction time. The synthesized Fe-IIPs exhibited an appropriate adsorption capacity of 134.224 mg g<sup>-1</sup>. In this study, the isotherm adsorption and kinetics study followed the Langmuir and pseudo-second order model. The selectivity of Fe-IIPs for Fe(III) in the presence of Cu(II) and Ni(II) were 1.059 for Fe/Cu and 1.086 for Fe/Ni. This study indicates that Fe-IIPs material can be applied for the preconcentration, separation, or removal of Fe(III) from complex matrices, contributing to analytical, environmental, and industrial applications.

## References

1. R. Yu, H. Yang, X. Yu, J. Cheng, X. Wang, H. Song, Y. Tan, H. Li, *Sep. Purif. Technol.*, **334**, 125985 (2024)
2. S. Satyam, S. Patra, *Heliyon*, **10**, 9 (2024)
3. M. M. Lazar, C. A. Ghioghita, E. S. Dragan, D. Humelnicu, M. V. Dinu, *Molec*, **28**, 6 (2023)
4. B. Ara, M. Muhammad, M. Salman, R. Ahmad, N. Islam, T. ul H. Zia, *Appl. Water Sci.*, **8**, 1 (2018)
5. W. Darmawan, D. A. Nurani, D. U. C. Rahayu, I. Abdullah, *AIP Conf. Proc.*, **2242**, 1 (2020)
6. M. C. Djunaidi, A. Q. Aini, D. S. Widodo, R. A. Lusiana, A. Suseno, *J. Phys. Conf. Ser.*, **1943**, 1 (2021)
7. R. Sharma, A. Kamal, R. K. Mahajan, *Soft Matter*, **12**, 6 (2016)
8. M. Behbahani, M. Taghizadeh, A. Bagheri, H. Hosseini, M. Salarian, A. Tootoonchi, *Microchim. Acta*, **178**, 432 (2012)

9. A. Karrat, J. J. García-Guzmán, J. M. Palacios-Santander, A. Amine, L. Cubillana-Aguilera, *Sensor Actuators B. Chem.*, **386**, 133751 (2023)
10. Y. Sui, S. Gao, J. Qi, S. Abliz, L. Chai, *Polymers (Basel)*, **17**, 229 (2025)
11. L. Al Sheakh, T. Niemann, A. Villinger, P. Stange, D. H. Zaitsau, A. Strate, R. Ludwig, *ChemPhysChem*, **22**, 1850-1856 (2021)
12. N. A. Zulkefli, W. E. F. W. Khalid, *Malaysian J. Chem.*, **26**, 3 (2024)
13. T. Bakalár, M. Kaňuchová, A. Girová, H. Pavolová, R. Hromada, Z. Hajduová, *Int. J. Environ. Res. Public Health*, **17**, 16 (2020)
14. P. Hadi, J. Barford, G. McKay, *Chem. Eng. J.*, **228**, 144 (2013)
15. K. Sinha, S. S. Sangani, A. D. Kehr, G. S. Rule, L. Jen-Jacobson, *Biochemistry*, **55**, 44 (2016)